Approximate Approximations

Vladimir Maz'ya

Gunther Schmidt

Department of Mathematics, Ohio State University, 231 W 18th Avenue, Columbus, OH 43210, USA

Department of Mathematical Sciences, M&O Building, University of Liverpool, Liverpool L69 3BX, UK

Department of Mathematics, University of Linköping, 581 83 Linköping, Sweden
E-mail address: vlmaz@mai.liu.se

Weierstrass Institute for Applied Analysis and Stochastics, Mohrenstr. 39, 10117 Berlin, Germany
E-mail address: schmidt@wias-berlin.de

2000 *Mathematics Subject Classification.* Primary 41A30

Key words and phrases. multivariate approximation, cubature of integral and pseudodifferential operators, approximate wavelets, numerical solution of integro-differential equations

Abstract. In this book realizations and applications of a new concept of approximation procedures are discussed. These procedures have the common feature that they are accurate without being convergent as the mesh size tends to zero.

The lack of convergence is compensated for by the flexibility in the choice of approximating functions, by the simplicity of the multi-dimensional generalization and by the possibility to obtain explicit formulas for values of various integral and pseudodifferential operators applied to the approximating functions.

This allows to design new classes of high order cubature formulas of integral and pseudodifferential operators and to develop new efficient numerical and semi-analytic methods for solving boundary value problems of mathematical physics.

Contents

Preface

• **General idea and motivation**. In this book, we discuss realizations and applications of a new concept of approximation procedures, called *approximate approximations*. Most of these procedures, which include approximate quasi-interpolation, interpolation, least square approximation, cubature of integral operators, and wavelet approximations, have one common feature. They are accurate without being convergent in a rigorous sense. In numerical mathematics, such a situation is not exceptional. For instance, non-convergent algorithms are natural in solving overdetermined ill-posed problems. However, for the approximation processes mentioned above, convergence is required.

Needless to say, the engineers and researchers who use numerical methods for solving applied problems do not need the convergence of the method. In fact, they need results, which are exact within a prescribed accuracy, determined mainly by the tolerance of measurements and other physical parameters, and always by the precision of the computing system. Their attitude, supported by common sense, was a powerful motivation for the development of our theory.

The lack of convergence in approximate approximations is compensated for, first of all, by the flexibility in the choice of basis functions and by the simplicity of the multi-dimensional generalization. Another, and probably the most important, advantage is the possibility of obtaining explicit formulas for values of various integral and pseudodifferential operators of mathematical physics applied to the basis functions.

The concept of approximate approximations and first related results were published by the first author in [**62**] – [**64**]. Later on, various aspects of a general theory of these approximations were systematically investigated in several joint papers by the authors ([**66**] – [**70**]). The present book is essentially based on the papers just mentioned and on our recent unpublished results. We also report on computational algorithms of the approximate approximations developed together with V. Karlin, T. Ivanov, W. Wendland, F. Lanzara, A. B. Movchan, *et al.*

The theory under consideration is at the very beginning of its development and we wrote this book with the hope of attracting new researchers to this area.

• **Approximate quasi-interpolation**. To give an impression of what we have in mind, recall, for example, that a typical error estimate of spline interpolation $M_h u$ on a uniform grid with size h, for a function $u \in C^N$, has the form

$$\|u - M_h u\|_C \leq c h^N \|u\|_{C^N}$$

with some integer N and a constant c independent of u and h. Here C and C^N are the spaces of continuous and N-times continuously differentiable functions.

In contrast to this situation, we fix $\varepsilon > 0$ and construct an *approximate quasi-interpolant* $M_{h,\varepsilon}u$ using the translates of a more or less arbitrary function η_ε instead of piecewise polynomials

$$M_{h,\varepsilon}u(x) = \sum_m u(hm)\eta_\varepsilon(x/h - m) \; .$$

One can show that

$$\|u - M_{h,\varepsilon}u\|_C \leq c_1(u)h^N + c_2(u)\,\varepsilon \, .$$

Thus, the error consists of a part converging with order N to zero as $h \to 0$ and a non-convergent part $c_2(u)\varepsilon$ called the *saturation error*. Thus, the procedure provides good approximations up to some prescribed error level, but it does not converge as $h \to 0$.

The approximate quasi-interpolation procedure can be extended to the approximation of functions on domains and manifolds with nonuniformly distributed nodes.

• **Cubature formulas**. The numerical treatment of potentials and other integral operators with singular kernels arises as a computational task in different fields. Since standard cubature methods are very time-consuming, there is ongoing research to develop new effective algorithms like panel clustering, multipole expansions or wavelet compression based on piecewise polynomial approximations of the density. The effective treatment of integral operators is also one of the main applications of approximate approximation.

The richness of the class of generating functions η makes it easier to find approximations for which the action of a given pseudodifferential operator can be effectively determined. For example, suppose one has to evaluate the convolution with a singular radial kernel as in the case of many potentials in mathematical physics. If the density is replaced by a quasi-interpolant with radial η, then after passing to spherical coordinates, the convolution is approximated by one-dimensional integrals. For many important integral operators $\mathcal{K}$ one can choose η even such that $\mathcal{K}\eta$ is analytically known, which results in semi-analytic cubature formulas for these operators. The special structure of the quasi-interpolation error gives rise to an interesting effect. Since the saturation error is a fast oscillating function and converges weakly to zero, the cubature formulas for potentials converge even in the rigorous sense, although there is no convergence for their densities.

• **Approximate wavelets**. Another example of approximate approximations is the notion of *approximate wavelet* decompositions for spaces generated by smooth functions satisfying refinement equations with a small error. It appears that those *approximate refinement equations* are satisfied by a broad class of scaling functions. This relation allows one to perform an approximate multi-resolution analysis of spaces generated by those functions. Therefore a wavelet basis can be constructed in which elements of fine scale spaces are representable within a given tolerance. The approximate wavelets provide most of the properties utilized in wavelet-based numerical methods and possess additionally simple analytic representations. Therefore the sparse approximation of important integral operators in the new basis can be computed using special functions or simple quadrature. One can give explicit formulas for harmonic and diffraction potentials whose densities are approximate wavelets.

• **Applications in mathematical physics**. The capability of approximate approximations to treat multi-dimensional integral operators enables one to develop new efficient numerical and semi-analytic methods for solving various problems in mathematical physics. First of all, this tool can be effectively used as an underlying approximation method in numerical algorithms for solving problems with integro-differential equations. Another very important application of approximate approximations is in the large field of integral equation methods for solving initial and boundary value problems for partial differential equations.

• **Structure of the book**. We describe briefly the contents of the book. More details are given in the introduction of each chapter. Most of the references to the literature are collected in Notes at the end of Chapters 2 - 13.

In Chapters 1 and 2 we analyze the approximate quasi-interpolation on uniform lattices. We start with simplest examples of second- and higher-order quasi-interpolants in both the one-dimensional and multi-dimensional cases. Then we turn to pointwise and integral error estimates for quasi-interpolation of functions given on the whole space. We formulate conditions on the generating functions η of quasi-interpolation formulas which ensure the smallness of saturation errors and the convergence with a given order up to the saturation bound.

A variety of basis functions and algorithms for their construction are the subject of Chapter 3. We provide examples giving rise to new classes of simple multivariate quasi-interpolation formulas which behave in numerical computations like high-order approximations.

Chapters 4 and 5 are dedicated to semi-analytic cubature formulas for numerous integral and pseudodifferential operators of mathematical physics, in particular for harmonic, elastic, and diffraction potentials. In Chapter 6 we obtain approximations of the inverse operator of the Cauchy problem for the heat, wave, and plate equations. There we also give formulas for the value of integral operators applied to more general basis functions.

The Gaussian functions possess remarkable approximation properties. Chapter 7 is devoted to quasi-interpolation and interpolation with these basis functions.

In Chapter 8 we perform approximate multi-resolution analysis for spaces generated by functions of the Schwartz class and introduce approximate wavelets. For the example of the Gaussian kernel we give simple analytic formulas of such wavelets first in the one-dimensional case and then in the case of many dimensions. We obtain quadratures of Newton and diffraction potentials acting on these wavelets.

in Chapter 9 the method of cubature of potentials is extended to the computation of these potentials over a bounded domain. Here we use mesh refinement towards the boundary of the domain and construct special boundary layer approximations. Our algorithm relies heavily on approximate refinement equations which, as was mentioned, play a crucial role in the construction of approximate wavelets also.

The approximate quasi-interpolation is extended in Chapter 10 to the approximation of functions on non-cubic grids and on domains and manifolds with non-uniformly distributed nodes.

In Chapter 11 we study approximate quasi-interpolation of scattered data. We show that simple modifications of basis functions provide an approximate partition of unity which allows the construction of high-order approximate quasi-interpolants on scattered centers.

Finally, in Chapters 12 and 13, we treat applications of approximate approximations to numerical algorithms of solving linear and non-linear pseudodifferential equations of mathematical physics. To be more specific, in Chapter 12 we apply the cubature methods developed in Chapter 4 to the solution of Lippmann-Schwinger type equations of scattering theory. We describe the Boundary Point Method, the application of approximate approximations to the solution of boundary integral equations. The same chapter contains formulas for the harmonic single layer potential acting on basis functions given on a surface. In Chapter 13, we describe applications to non-linear evolution equations with local and non-local operators, including the Navier-Stokes, Joseph, Benjamin-Ono, and Sivashinsky equations.

• **Readership**. The book is intended for graduate students and researchers interested in applied approximation theory and numerical methods for solving problems of mathematical physics. No special knowledge is required to read this book, except for conventional university courses on functional analysis and numerical methods.

•**Acknowledgments**. The authors would like to thank F. Lanzara, V. Karlin, and T. Ivanov for the help in obtaining some of the numerical results presented in the book.

This research was made possible by support from DAAD and Svenska institutet (grant 313/S-PPP 4/96) and INTAS (grant 97-30551). The first author was partially supported by the NSF grant DMS 0500029. The second author was partially supported within the DFG Priority Program 1095. Both authors want to thank the Department of Mathematics of the University of Rome "La Sapienza" for the warm hospitality, and the second author gratefully ackknowledges the hospitality of the Department of Mathematical Sciences at the University of Liverpool.

V. Maz′ya and G. Schmidt

CHAPTER 1

Quasi-interpolation

1.1. Introduction

1.1.1. Exercise for a freshman. Suppose we are given the task of drawing the graph of the function

$$f(x) = \sum_{m=-\infty}^{\infty} \mathrm{e}^{-(x-m)^2/2}$$

obtained by summation of shifted Gaussians, which are depicted in Fig. 1.1.

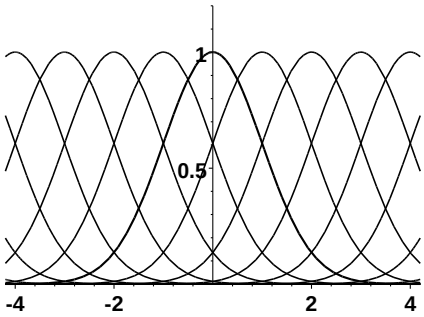

FIGURE 1.1

The function $f(x)$ is, of course, bounded, positive, and smooth. Moreover, $f(x+1) = f(x)$, i.e., it is periodic with period 1. So we expect that the graph of f should look like a nice periodic wavy curve. However, it is quite astonishing to find out that this graph, which can be easily produced with standard plotting software and which is depicted in Fig. 1.2, is a constant.

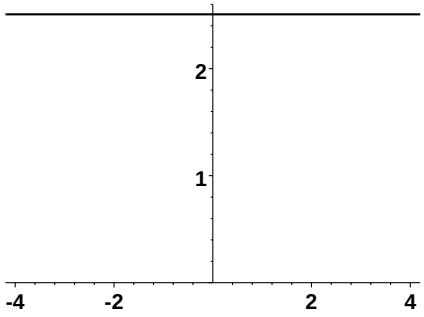

FIGURE 1.2. Graph of $f(x)$

In fact, this superficial impression proves to be wrong. If the scale of the y-axis is changed as in Fig. 1.3, then we see that $f(x)$ is not constant; it oscillates between 2.50662826 and 2.50662829.

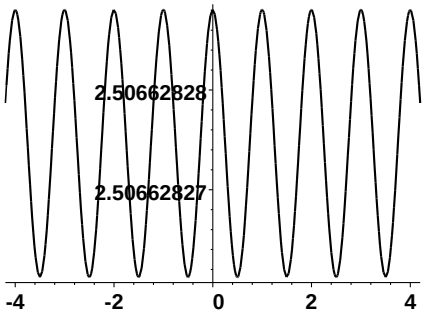

FIGURE 1.3. Zoomed graph of $f(x)$

One obtains the same picture if this procedure is repeated for the sum

$$f_{\mathcal{D}}(x) = \sum_{m=-\infty}^{\infty} \mathrm{e}^{-(x-m)^2/\mathcal{D}}$$

with different values of the parameter $\mathcal{D} > 0$. Figs. 1.4 and 1.5 show the graph of $f_{\mathcal{D}}$ for the parameters $\mathcal{D} = 0.5$ and $\mathcal{D} = 4$, respectively. The plot of the function

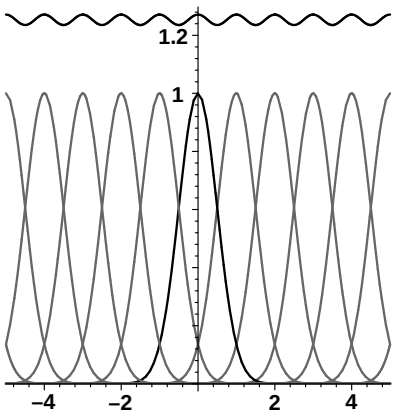

FIGURE 1.4. $f_{1/2}(x)$ and individual terms

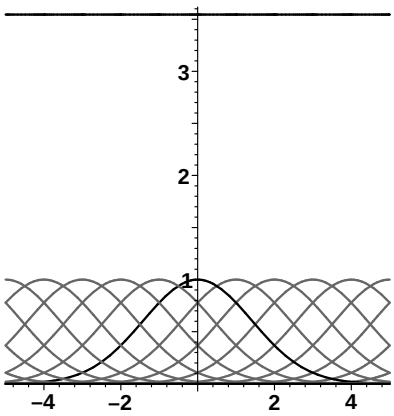

FIGURE 1.5. $f_4(x)$ and individual terms

$f_{1/2}(x)$ shows the oscillating behavior, whereas f_4 looks like a constant. In fact f_4 is also oscillating between $3.54490770181103205 \pm 1.43 \cdot 10^{-15}$, which is very hard to depict. One can conjecture, that the oscillating function $f_{\mathcal{D}}$ tends to a constant if $\mathcal{D}$ increases.

To rigorously explain peculiarities of the graphs, let us consider the Fourier series of the function

$$\theta(x,\mathcal{D}) = \frac{1}{\sqrt{\pi\mathcal{D}}} \sum_{m=-\infty}^{\infty} \mathrm{e}^{\,-(x-m)^2/\mathcal{D}}\,,\ \mathcal{D}>0\,. \tag{1.1}$$

Its coefficients can be computed as follows:

$$\begin{aligned}
&\frac{1}{\sqrt{\pi\mathcal{D}}} \int_0^1 \sum_{m=-\infty}^{\infty} \mathrm{e}^{\,-(x-m)^2/\mathcal{D}}\ \mathrm{e}^{\,-2\pi i\nu x}\ dx = \frac{1}{\sqrt{\pi\mathcal{D}}} \sum_{m=-\infty}^{\infty} \int_m^{m+1} \mathrm{e}^{\,-x^2/\mathcal{D}}\ \mathrm{e}^{\,-2\pi i\nu x}\ dx \\
&= \frac{1}{\sqrt{\pi\mathcal{D}}} \int_{-\infty}^{\infty} \mathrm{e}^{\,-x^2/\mathcal{D}}\ \mathrm{e}^{\,-2\pi i\nu x}\ dx = \frac{\mathrm{e}^{\,-\pi^2\mathcal{D}\nu^2}}{\sqrt{\pi\mathcal{D}}} \int_{-\infty}^{\infty} \mathrm{e}^{\,-(x/\sqrt{\mathcal{D}}+i\pi\sqrt{\mathcal{D}}\nu)^2}\ dx \\
&= \frac{\mathrm{e}^{\,-\pi^2\mathcal{D}\nu^2}}{\sqrt{\pi\mathcal{D}}} \int_{-\infty}^{\infty} \mathrm{e}^{\,-x^2/\mathcal{D}}\ dx = \mathrm{e}^{\,-\pi^2\mathcal{D}\nu^2}\,.
\end{aligned}$$

The order of summation and integration can be changed here because of the absolute convergence of the infinite sum. Hence we obtain the Fourier series

$$\theta(x,\mathcal{D}) = \sum_{\nu=-\infty}^{\infty} \mathrm{e}^{\,-\pi^2\mathcal{D}\nu^2}\ \mathrm{e}^{\,2\pi i\nu x}\,. \tag{1.2}$$

This representation of the function θ is a special case of the so-called Poisson summation formula

$$\sum_{m=-\infty}^{\infty} u(x+m) = \sum_{\nu=-\infty}^{\infty} \mathcal{F}u(\nu)\ \mathrm{e}^{\,2\pi i\nu x}\,, \tag{1.3}$$

where $\mathcal{F}u$ denotes the Fourier transform of the function u. The definition of the Fourier transform will be given in Section 2.1, where we also discuss some properties of this important formula.

From (1.2), we have

$$\theta(x,\mathcal{D}) = 1 + 2\sum_{\nu=1}^{\infty} \mathrm{e}^{-\pi^2\mathcal{D}\nu^2} \cos 2\pi\nu x\,,$$

i.e., our function $\theta(x,\mathcal{D})$ differs from 1 by the infinite series

$$2\sum_{\nu=1}^{\infty} \mathrm{e}^{-\pi^2\mathcal{D}\nu^2} \cos 2\pi\nu x\,. \tag{1.4}$$

The coefficients $\mathrm{e}^{-\pi^2\mathcal{D}\nu^2}$, $\nu = 1, 2, \ldots$, can be very small depending on $\mathcal{D}$, as seen from the relation $\mathrm{e}^{-\pi^2} = 0.000051723\ldots$. In particular, if $\mathcal{D} \geq 1$, then for any x the modulus of (1.4) is less than $1.04 \cdot 10^{-4\mathcal{D}}$. Note that in the cases $\mathcal{D} = 2$ and $\mathcal{D} = 4$ the difference is comparable to the single and, respectively, double precision in the arithmetics of most modern computers, i.e., in these cases where the function $\theta(x,\mathcal{D})$ is numerically the constant function 1. Moreover, the difference $|\theta(x,\mathcal{D}) - 1|$ can be made less than any prescribed positive tolerance ε by choosing $\mathcal{D}$ large enough. For this it suffices to take

$$\mathcal{D} > \pi^{-2}(\log|\varepsilon| - \log 2)\,.$$

REMARK 1.1. The function θ is closely connected with Jacobi's Theta function ϑ_3, which is defined as (see [**1**, 16.27])

$$\vartheta_3(z|\tau) := \sum_{n=-\infty}^{\infty} \mathrm{e}^{\,i\pi\tau n^2}\,\mathrm{e}^{\,2inz}\,, \tag{1.5}$$

by the relation $\theta(x,\mathcal{D}) = \vartheta_3(\pi x|i\pi\mathcal{D})$.

1.1.2. Simple approximation formula. We have seen that for "large" $\mathcal{D}$ the integer shifts

$$\left\{\frac{1}{\sqrt{\pi\mathcal{D}}}\ \mathrm{e}^{-(x-m)^2/\mathcal{D}}, m\in\mathbb{Z}\right\} \tag{1.6}$$

form an approximate partition of unity, i.e., the sum of these functions is approximatively equal to the constant function 1. In addition, the functions in the family (1.6) decay very rapidly if $|x-m|\to\infty$. Hence, in the sum (1.1), one has to take into account only a small number of terms, if one wants to compute the value at a given point x. This leads to the idea of introducing an approximation formula using the usual scaling and translation operations with a "small" parameter h for the family of functions $\mathrm{e}^{-x^2/\mathcal{D}}$

$$\mathcal{M}_{h,\mathcal{D}}u(x) = \frac{1}{\sqrt{\pi\mathcal{D}}}\sum_{m=-\infty}^{\infty} u(mh)\ \mathrm{e}^{\,-(x-mh)^2/\mathcal{D}h^2}\ . \tag{1.7}$$

Formulas of this type are known as *quasi-interpolants* and we are interested in their behavior as $h\to 0$.

Let us suppose that the function u is twice continuously differentiable with bounded derivatives. The Taylor expansion of u at the point mh has the form

$$u(mh) = u(x) + u'(x)(mh-x) + u''(x_m)\frac{(mh-x)^2}{2}$$

for some x_m between x and mh. Putting this into (1.7), we derive

$$\begin{aligned}\mathcal{M}_{h,\mathcal{D}}u(x) = {}& \frac{u(x)}{\sqrt{\pi\mathcal{D}}}\sum_{m=-\infty}^{\infty}\mathrm{e}^{-(x-mh)^2/\mathcal{D}h^2}\\ &+\frac{u'(x)}{\sqrt{\pi\mathcal{D}}}\sum_{m=-\infty}^{\infty}(mh-x)\ \mathrm{e}^{-(x-mh)^2/\mathcal{D}h^2}\\ &+\frac{1}{2\sqrt{\pi\mathcal{D}}}\sum_{m=-\infty}^{\infty}u''(x_m)(mh-x)^2\ \mathrm{e}^{-(x-mh)^2/\mathcal{D}h^2}\,.\end{aligned} \tag{1.8}$$

The sum of the first term on the right-hand side is the function $\theta(x/h,\mathcal{D})$, whereas the sum in the second term can be expressed, for example, by the derivative

$$\theta'\big(\frac{x}{h},\mathcal{D}\big) = \frac{2}{\sqrt{\pi\mathcal{D}}\mathcal{D}h}\sum_{m=-\infty}^{\infty}(mh-x)\ \mathrm{e}^{-(x-mh)^2/\mathcal{D}h^2},$$

which provides the relation

$$\frac{1}{\sqrt{\pi\mathcal{D}}}\sum_{m=-\infty}^{\infty}(mh-x)\ \mathrm{e}^{-(x-mh)^2/\mathcal{D}h^2} = -2\pi\mathcal{D}h\sum_{\nu=1}^{\infty}\nu\,\mathrm{e}^{-\pi^2\mathcal{D}\nu^2}\sin 2\pi\nu\frac{x}{h}\,.$$

Therefore, by using (1.2), we can write the quasi-interpolant in the form

$$\mathcal{M}_{h,\mathcal{D}}u(x) = u(x) + C_{\mathcal{D},h}(x) + R_h(x) \tag{1.9}$$

with the function

$$C_{\mathcal{D},h}(x) = 2u(x)\sum_{\nu=1}^{\infty} \mathrm{e}^{-\pi^2\mathcal{D}\nu^2}\cos 2\pi\nu\frac{x}{h} - 2u'(x)\pi\mathcal{D}h\sum_{\nu=1}^{\infty}\nu\,\mathrm{e}^{-\pi^2\mathcal{D}\nu^2}\sin 2\pi\nu\frac{x}{h} \tag{1.10}$$

and the remainder term

$$R_h(x) = \frac{1}{2\sqrt{\pi\mathcal{D}}}\sum_{m=-\infty}^{\infty} u''(x_m)(mh-x)^2\ \mathrm{e}^{-(x-mh)^2/\mathcal{D}h^2},$$

which obviously satisfies

$$|R_h(x)| \le \max_{t\in\mathbb{R}}|u''(t)|\,\frac{1}{2\sqrt{\pi\mathcal{D}}}\sum_{m=-\infty}^{\infty}(mh-x)^2\ \mathrm{e}^{-(x-mh)^2/\mathcal{D}h^2}.$$

The Fourier series of the last sum can be calculated similarly to the case $\theta(x,\mathcal{D})$, and it holds that

$$\frac{1}{\sqrt{\pi\mathcal{D}}}\sum_{m=-\infty}^{\infty}(mh-x)^2\,\mathrm{e}^{-(x-mh)^2/\mathcal{D}h^2} = \frac{\mathcal{D}h^2}{2}\sum_{\nu=-\infty}^{\infty}(1-2\pi^2\mathcal{D}\nu^2)\,\mathrm{e}^{-\pi^2\mathcal{D}\nu^2}\,\mathrm{e}^{2\pi i\nu x/h},$$

which leads to the estimate

$$|R_h(x)| \le \max_{t\in\mathbb{R}}|u''(t)|\frac{\mathcal{D}h^2}{4}\Big(1+2\sum_{\nu=1}^{\infty}\Big|(1-2\pi^2\mathcal{D}\nu^2)\cos 2\pi\nu\frac{x}{h}\Big|\,\mathrm{e}^{-\pi^2\mathcal{D}\nu^2}\Big).$$

Hence, the difference between u and the quasi-interpolant $\mathcal{M}_{h,\mathcal{D}}u$ can be estimated for any $x\in\mathbb{R}$ by

$$\begin{aligned}\big|\mathcal{M}_{h,\mathcal{D}}u(x) - u(x)\big| \le\ & \frac{\mathcal{D}h^2}{4}\big(1+\sum_{\nu=1}^{\infty}|4\pi^2\mathcal{D}\nu^2-2|\,\mathrm{e}^{-\pi^2\mathcal{D}\nu^2}\big)\max_{t\in\mathbb{R}}|u''(t)| \\ & + \big|C_{\mathcal{D},h}(x)\big|.\end{aligned} \tag{1.11}$$

This inequality is valid for all values of the positive parameters $\mathcal{D}$ and h. Here we find the special feature of approximate approximations, mentioned in the Preface. The approximation error consists of a term of the order $\mathcal{O}(\mathcal{D}h^2)$ and the term $\big|C_{\mathcal{D},h}(x)\big|$, which is called the *saturation error*, because it does not converge to zero as $h\to 0$. However, we obtain from (1.10) that

$$\big|C_{\mathcal{D},h}(x)\big| \le 2|u(x)|\sum_{\nu=1}^{\infty}\mathrm{e}^{-\pi^2\mathcal{D}\nu^2} + 2\pi\mathcal{D}h|u'(x)|\sum_{\nu=1}^{\infty}\nu\,\mathrm{e}^{-\pi^2\mathcal{D}\nu^2}.$$

Therefore, owing to the rapid decay of $\mathrm{e}^{-\pi^2\mathcal{D}\nu^2}$, $\nu=1,2,\ldots$, for any $\varepsilon>0$ one can fix $\mathcal{D}>0$ such that the saturation error satisfies

$$|C_{\mathcal{D},h}(x)| < \varepsilon\,\big(|u(x)| + h|u'(x)|\big).$$

Since the first term of the right-hand side of (1.11) with a fixed $\mathcal{D}$ converges to zero, we see that $\mathcal{M}_{h,\mathcal{D}}u$ approximates u with the order $\mathcal{O}(h^2)$ as long as the saturation bound $\varepsilon\big(|u(x)|+h|u'(x)|\big)$ is reached. Hence, choosing the parameter $\mathcal{D}$ such that

ε is less than the precision of the computing system, formula $\mathcal{M}_{h,\mathcal{D}}u$ behaves in numerical computations as a usual second-order approximation.

Let us emphasize the structure of $C_{\mathcal{D},h}$, which is the sum of $u(x)$ and $hu'(x)$ multiplied by oscillating functions with period h. For sufficiently large $\mathcal{D}$ the main term of $C_{\mathcal{D}}$ is given by

$$2u(x)\,\mathrm{e}^{\,-\pi^2\mathcal{D}}\cos 2\pi\frac{x}{h}\,.$$

This is a fast oscillating simple harmonics modulated by the slowly varying value of the approximated function.

In the following we show that formulas of type (1.7), where the Gaussian $\mathrm{e}^{\,-x^2}$ is replaced by more general basis functions, can provide similar or even better approximation properties. We give some one- and multi-dimensional examples of those approximation formulas and define approximate quasi-interpolation on uniform grids in the next section.

1.2. Further examples

1.2.1. Errors of approximate quasi-interpolation. We illustrate here the approximation properties of the quasi-interpolant $\mathcal{M}_{h,\mathcal{D}}u$ defined in (1.7) for the function $u(x)=\sin x$ using different values of the parameters $\mathcal{D}$ and h. Figs. 1.6 and 1.7 show the particular form of the terms

$$\frac{1}{\sqrt{\pi\mathcal{D}}}\,\sin(mh)\;\mathrm{e}^{\,-(x-mh)^2/\mathcal{D}h^2} \tag{1.12}$$

and its sum

$$(\mathcal{M}_{h,\mathcal{D}}\sin)(x)=\frac{1}{\sqrt{\pi\mathcal{D}}}\sum_{m=-\infty}^{\infty}\sin(mh)\;\mathrm{e}^{\,-(x-mh)^2/\mathcal{D}h^2} \tag{1.13}$$

for $h=0.4$ and two different values $\mathcal{D}=1$ and $\mathcal{D}=2$. Visually the sums are good approximations of $\sin x$ for this rather large step h.

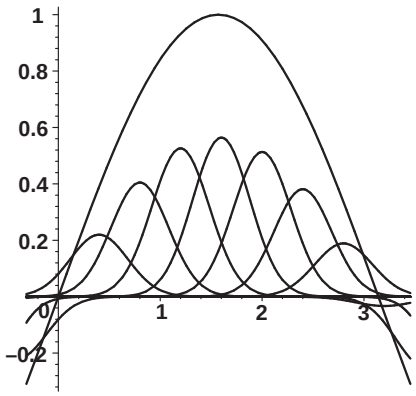

FIGURE 1.6. $\mathcal{D}=1$, $h=0.4$

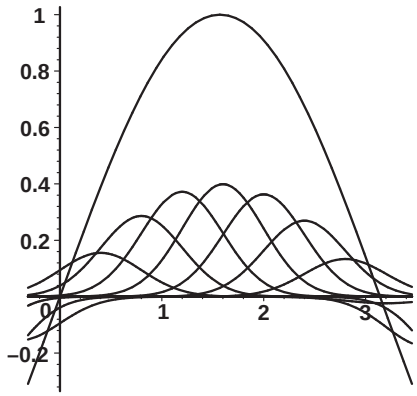

FIGURE 1.7. $\mathcal{D}=2$, $h=0.4$

Although the functions $\mathrm{e}^{-(x-mh)^2/\mathcal{D}h^2}$ are supported by the whole real axis, one needs only a few terms in the sum (1.7) to compute the value of $\mathcal{M}_{h,\mathcal{D}}u$ at a

given point x within a given accuracy. For a fixed tolerance $\delta > 0$ one has to sum only over the integers m for which

$$|m - x/h| \le \sqrt{-\mathcal{D}\log\delta}\,.$$

Hence the number of terms, necessary to compute $\mathcal{M}_{h,\mathcal{D}}u(x)$ for fixed h, increases proportionally to $\sqrt{\mathcal{D}}$.

On the other hand, if $\mathcal{D}$ is fixed, then this number does not depend on h. For example, if $\delta = 10^{-6}$, then one has to sum up 7 and 11 terms in (1.7) if $\mathcal{D} = 1$ and $\mathcal{D} = 2$, respectively.

The differences between $\sin x$ and the quasi-interpolants (1.13) are plotted in Figs. 1.8 and 1.9 for the values $\mathcal{D} = 1, 2$ and $h = 0.4, 0.2$, respectively. The graphs confirm the second-order convergence from estimate (1.11). However, the case of

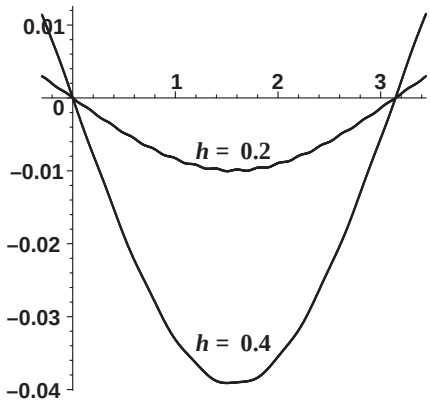

FIGURE 1.8. $(\mathcal{M}_{h,1} - I)\sin x$

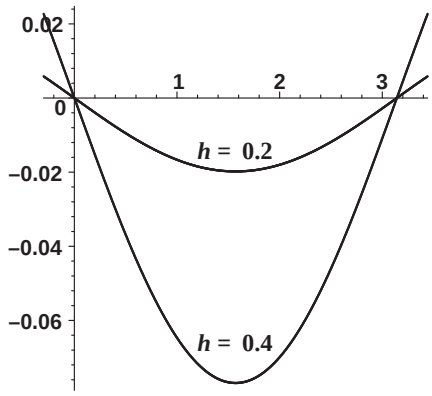

FIGURE 1.9. $(\mathcal{M}_{h,2} - I)\sin x$

smaller step h already gives different pictures. Figs. 1.10–1.15 depict the quasi-interpolation error of $\sin x$ with smaller h and for $\mathcal{D} = 1$ and 2.

The plotted errors confirms the second-order convergence, but the error for $\mathcal{D} = 1$ oscillates very fast, with frequency depending of h. In Figs. 1.10 and 1.12 the saturation error is already visible.

It can be seen from Fig. 1.14, that for $\mathcal{D} = 1$ the quasi-interpolation error has reached its saturation bound, since it does not decrease if h becomes smaller. On the other hand, Fig. 1.15 shows that the approximation with $\mathcal{M}_{h,2}$ for the same values of h is of the second order, that the saturation is not reached, yet.

The behavior of the quasi-interpolants $\mathcal{M}_{h,\mathcal{D}}$, predicted by the estimate (1.11), is confirmed also in Table 1.1, where the quasi-interpolation error in the maximum norm for different h and $\mathcal{D}$ and the convergence rate calculated as

$$\log_2 \frac{\|u - \mathcal{M}_{2h,\mathcal{D}}u\|_{L^\infty}}{\|u - \mathcal{M}_{h,\mathcal{D}}u\|_{L^\infty}} \tag{1.14}$$

are given.

Recall that the main term of the saturation error is $1.04\cdot 10^{-4\mathcal{D}}\,|u(x)|$. If $\mathcal{D} = 1$, then we have the second-order approximation only for relative large h. In the cases

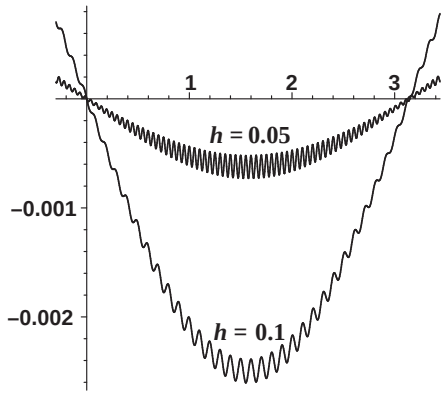

FIGURE 1.10. $(\mathcal{M}_{h,1} - I)\sin x$

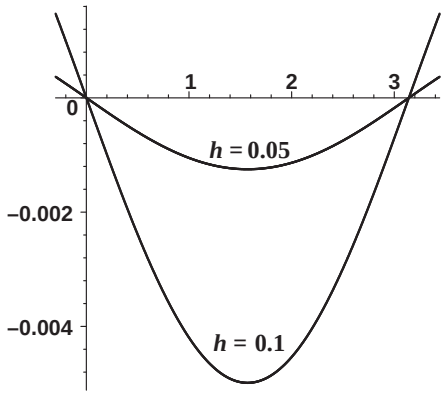

FIGURE 1.11. $(\mathcal{M}_{h,2} - I)\sin x$

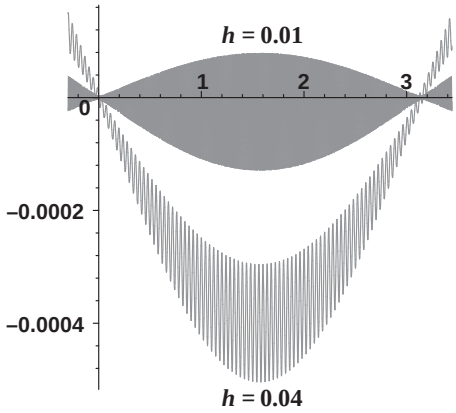

FIGURE 1.12. $(\mathcal{M}_{h,1} - I)\sin x$

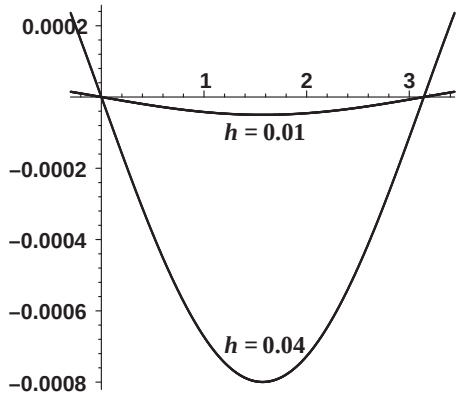

FIGURE 1.13. $(\mathcal{M}_{h,2} - I)\sin x$

$\mathcal{D} = 2$ and $\mathcal{D} = 4$ the saturation error is still negligible compared to the first term of estimate (1.11).

1.2.2. A simple application of the approximation formula (1.7)**.** Consider the initial value problem for the heat equation

$$u_t(x,t) - u_{xx}(x,t) = 0\,, \quad t > 0\,, \quad u(x,0) = \varphi(x), \quad x \in \mathbb{R}\,. \tag{1.15}$$

Its solution is given by the *Poisson integral*

$$u(x,t) = \mathcal{P}_t\varphi(x) := \frac{1}{\sqrt{4\pi t}} \int_{\mathbb{R}} \mathrm{e}^{-(x-y)^2/4t}\, \varphi(y)\, dy\,.$$

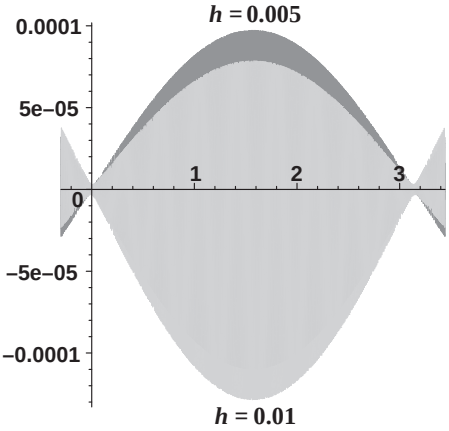

FIGURE 1.14. $(\mathcal{M}_{h,1} - I)\sin x$

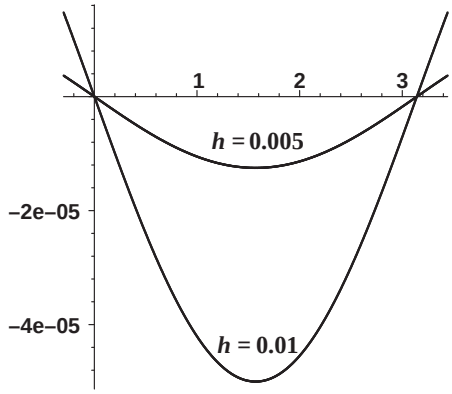

FIGURE 1.15. $(\mathcal{M}_{h,2} - I)\sin x$

h	$\mathcal{D}=1$	rate	$\mathcal{D}=2$	rate	$\mathcal{D}=4$	rate
0.4	$3.91\cdot 10^{-2}$		$7.69\cdot 10^{-2}$		$1.48\cdot 10^{-1}$	
0.2	$1.00\cdot 10^{-2}$	1.96	$1.98\cdot 10^{-2}$	1.96	$3.92\cdot 10^{-2}$	1.91
0.1	$2.60\cdot 10^{-3}$	1.95	$4.99\cdot 10^{-3}$	1.99	$9.95\cdot 10^{-3}$	1.98
0.05	$7.29\cdot 10^{-4}$	1.84	$1.25\cdot 10^{-3}$	2.00	$2.50\cdot 10^{-3}$	1.99
0.025	$2.60\cdot 10^{-4}$	1.49	$3.12\cdot 10^{-4}$	2.00	$6.25\cdot 10^{-4}$	2.00
0.0125	$1.42\cdot 10^{-4}$	0.87	$7.81\cdot 10^{-5}$	2.00	$1.56\cdot 10^{-4}$	2.00
0.00625	$1.11\cdot 10^{-4}$	0.36	$1.95\cdot 10^{-5}$	2.00	$3.91\cdot 10^{-5}$	2.00

TABLE 1.1. Approximation error for the function $u(x) = \sin x$ using the quasi-interpolant (1.7)

This integral cannot be taken in a closed form, in general, but this is possible for some functions φ, for example, for the Gaussian function. In particular,

$$\frac{1}{\sqrt{4\pi t}} \int_{\mathbb{R}} \mathrm{e}^{-(x-y)^2/4t}\, \mathrm{e}^{-y^2/\mathcal{D}h^2}\, dy = \frac{\sqrt{\mathcal{D}}h}{\sqrt{\mathcal{D}h^2+4t}}\, \mathrm{e}^{-x^2/(\mathcal{D}h^2+4t)}\,. \tag{1.16}$$

Hence, if we replace the initial value φ by the quasi-interpolant $\mathcal{M}_{h,\mathcal{D}}\varphi$ defined by (1.7), then we obtain the exact solution

$$\mathcal{P}_t(\mathcal{M}_{h,\mathcal{D}}\varphi)(x) = \frac{h}{\sqrt{\pi(\mathcal{D}h^2+4t)}} \sum_{m=-\infty}^{\infty} \varphi(hm)\, \mathrm{e}^{-(x-hm)^2/(\mathcal{D}h^2+4t)} \tag{1.17}$$

of the heat equation (1.15) with the modified initial condition $u(x,0) = \mathcal{M}_{h,\mathcal{D}}\varphi(x)$. Since

$$\begin{aligned}\big|\mathcal{P}_t\varphi(x) - \mathcal{P}_t(\mathcal{M}_{h,\mathcal{D}}\varphi)(x)\big| &\le \sup_{y\in\mathbb{R}} \big|\varphi(y) - \mathcal{M}_{h,\mathcal{D}}\varphi(y)\big| \, \frac{1}{\sqrt{4\pi t}} \int_{\mathbb{R}} \mathrm{e}^{-(x-y)^2/4t}\, dy \\ &= \sup_{y\in\mathbb{R}} \big|\varphi(y) - \mathcal{M}_{h,\mathcal{D}}\varphi(y)\big| \,,\end{aligned}$$

the estimate (1.11) shows that the function $u_h(x,t) = \mathcal{P}_t(\mathcal{M}_{h,\mathcal{D}}\varphi)(x)$ approximates the solution $u(x,t)$ of the original problem (1.15) with the error

$$\begin{aligned}|u(x,t) - u_h(x,t)| \le{}& \frac{\mathcal{D}h^2}{4}\big(1 + 4\mathcal{D}\pi^2\,\mathrm{e}^{-\pi^2\mathcal{D}}\big) \max_{y\in\mathbb{R}} |\varphi''(y)| \\ &+ 2\max_{y\in\mathbb{R}} \big(|\varphi(y)| + |\varphi'(y)|\pi\mathcal{D}h\big)\,\mathrm{e}^{-\pi^2\mathcal{D}} + \mathcal{O}(\mathrm{e}^{-2\pi^2\mathcal{D}})\,.\end{aligned} \tag{1.18}$$

This very simple example is in many ways typical of the application of approximate approximations to the solution of partial differential equations; one replaces some function in the original problem by an approximant such that the solution of the equation can be performed very efficiently, either analytically or by some other numerical method.

Let us mention that (1.18) is only a rough error estimate for the approximate solution of the heat equation. This can be seen from Table 1.2 which contains numerical results for the heat equation (1.15) with the initial value $\phi(x) = \mathrm{e}^{-x^2}$. It provides the maximum error

$$\max_x |u(x,t) - u_h(x,t)|\,, \quad t = 10\,,$$

for different values of $\mathcal{D}$ and h.

h	$\mathcal{D}=1$	rate	$\mathcal{D}=2$	rate	$\mathcal{D}=4$	rate
0.4	$3.04\cdot10^{-4}$		$6.06\cdot10^{-4}$		$1.20\cdot10^{-3}$	
0.2	$7.61\cdot10^{-5}$	2.00	$1.52\cdot10^{-4}$	2.00	$3.04\cdot10^{-4}$	1.99
0.1	$1.90\cdot10^{-5}$	2.00	$3.81\cdot10^{-5}$	2.00	$7.61\cdot10^{-5}$	2.00
0.05	$4.76\cdot10^{-6}$	2.00	$9.52\cdot10^{-6}$	2.00	$1.90\cdot10^{-5}$	2.00
0.025	$1.19\cdot10^{-6}$	2.00	$2.38\cdot10^{-6}$	2.00	$4.76\cdot10^{-6}$	2.00
0.0125	$2.98\cdot10^{-7}$	2.00	$5.95\cdot10^{-7}$	2.00	$1.19\cdot10^{-6}$	2.00
0.00625	$7.44\cdot10^{-8}$	2.00	$1.49\cdot10^{-7}$	2.00	$2.98\cdot10^{-7}$	2.00

TABLE 1.2. Numerical error for the initial value problem (1.15) with $\phi(x) = \mathrm{e}^{-x^2}$ and $t = 10$ using the approximate solution (1.17)

In contrast to the quasi-interpolation results, given in Table 1.1, a saturation error cannot be seen. We will show in Subsection 6.2.1 that due to the properties of the Poisson integral and the structure of the saturation error the approximate solution $u_h(x,t)$ converges to $u(x,t)$.

1.2.3. Other basis functions. The simplicity of formulas of the form

$$\mathcal{Q}_h u(x) := \sum_{m=-\infty}^{\infty} u(mh)\,\eta\Big(\frac{x}{h} - m\Big) \tag{1.19}$$

makes them very attractive for approximation processes. Suppose, for example, that η is a *Lagrangian function*, which means that η is subject to

$$\eta(0) = 1 \quad \text{and} \quad \eta(m) = 0 \quad \text{for all } m \in \mathbb{Z}\backslash 0\,.$$

Then the sum (1.19) satisfies $\mathcal{Q}_h u(mh) = u(mh)$, $m \in \mathbb{Z}$, i.e., $\mathcal{Q}_h u$ interpolates u. As two representative examples, we mention here the piecewise linear hat function and the sinc function

$$\operatorname{sinc} x = \frac{\sin \pi x}{\pi x}\,.$$

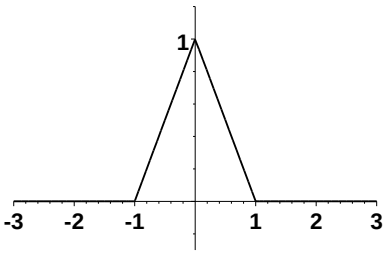

FIGURE 1.16. Hat function

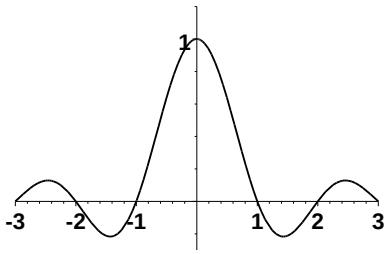

FIGURE 1.17. sinc function

If η is the hat function as shown in Fig. 1.16, then the resulting sum is the polygonal line connecting the points $(hm, u(hm))$. This piecewise linear function approximates u with the order $\mathcal{O}(h^2)$. To find the approximant at a given point x, one has to sum up only two terms of (1.19). But it is visually not very nice to approximate a smooth curve by some piecewise linear function.

On the other hand, the sinc function (depicted in Fig. 1.17) generates an interpolant which is smooth and even provides an exponential order of convergence (see [**91**]). However, since the generating function decreases very slowly, it is practically impossible to compute the approximant (1.19) if the function u is not compactly supported.

Let us mention that in Chapter 7 we introduce another Lagrangian function

$$\Psi_{\mathcal{D}}(x) = \frac{\sin \pi x}{\pi \mathcal{D} \sinh \dfrac{x}{\mathcal{D}}}$$

depending on the parameter $\mathcal{D} > 0$. This function is a small perturbation of the Lagrangian function from the family of shifted Gaussians (1.6). The corresponding interpolant approximates smooth functions with exponential order, but similar to the approximation formula (1.7) only up to a saturation error of the order $\mathcal{O}(\mathrm{e}^{-\pi^2 \mathcal{D}})$. Therefore $\Psi_{\mathcal{D}}$ can be considered as approximate sinc function, providing similar approximation properties but decaying exponentially for $|x| \to \infty$.

There exists, of course, a variety of other basis functions η for interpolation formulas (1.19). However, the Lagrangian functions for those bases have, in general, large supports. For example, the Lagrangian function for the class of smooth cubic splines, which are cubic polynomials on the intervals $(m, m+1)$, $m \in \mathbb{Z}$, and two-times continuously differentiable, is supported on the whole real line.

It turns out, that good approximations can be obtained also by replacing the Lagrangian function in (1.19) by some simpler function of the same class. In the case of smooth cubic splines one can choose η as the cubic B-spline

$$b(x) = \frac{1}{12}\big(|x+2|^3 - 4|x+1|^3 + 6|x|^3 - 4|x-1|^3 + |x-2|^3\big) \tag{1.20}$$

depicted in Fig. 1.18, which gives a C^2-approximant of the order $\mathcal{O}(h^2)$.

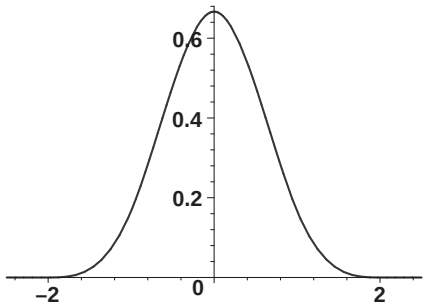

FIGURE 1.18. Cubic B-spline

But clearly the resulting approximant does not interpolate; therefore approximation formulas (1.19) with non-Lagrangian functions η are called *quasi-interpolants*.

Thus, $\mathcal{M}_{h,\mathcal{D}}$ in (1.7) represents a quasi-interpolant with

$$\eta(x) = \frac{\mathrm{e}^{-x^2/\mathcal{D}}}{\sqrt{\pi\mathcal{D}}}\,.$$

We have seen in (1.11) that for a fixed $\mathcal{D}$ the sum $\mathcal{M}_{h,\mathcal{D}}u$ is a smooth approximation to u of order $\mathcal{O}(h^2)$ until the saturation error is reached, which can be neglected in numerical computations if $\mathcal{D}$ is sufficiently large.

It is important that for a quite general class of basis functions the quasi-interpolants have similar properties as in the case of the Gaussian. Take, for example, the function

$$\operatorname{sech} x = \frac{1}{\cosh x}\,.$$

Putting the Taylor expansion of u into

$$\mathcal{M}_h u(x) = \frac{1}{\pi\sqrt{\mathcal{D}}} \sum_{m=-\infty}^{\infty} u(mh) \operatorname{sech} \frac{x-mh}{\sqrt{\mathcal{D}}h}\,, \tag{1.21}$$

we obtain as in (1.8)

$$\mathcal{M}_h u(x) = \frac{u(x)}{\pi\sqrt{\mathcal{D}}} \sum_{m=-\infty}^{\infty} \operatorname{sech} \frac{x-mh}{\sqrt{\mathcal{D}}h} + \frac{u'(x)}{\pi\sqrt{\mathcal{D}}} \sum_{m=-\infty}^{\infty} (mh-x) \operatorname{sech} \frac{x-mh}{\sqrt{\mathcal{D}}h}$$
$$+ \frac{1}{2\pi\sqrt{\mathcal{D}}} \sum_{m=-\infty}^{\infty} u''(x_m)(mh-x)^2 \operatorname{sech} \frac{x-mh}{\sqrt{\mathcal{D}}h}\,.$$

The infinite sums in the first and second term on the right-hand side can be transformed by using Poisson's summation formula (1.3) and the Fourier transform of $\operatorname{sech} x$,

$$(\mathcal{F}\operatorname{sech})(\lambda) = \pi \operatorname{sech} \pi^2 \lambda \,.$$

Then we obtain the relations

$$\begin{aligned} I_0 &:= \frac{1}{\pi\sqrt{\mathcal{D}}} \sum_{m=-\infty}^{\infty} \operatorname{sech} \frac{x-m}{\sqrt{\mathcal{D}}} = 1 + 2\sum_{\nu=1}^{\infty} \operatorname{sech}(\pi^2\sqrt{\mathcal{D}}\nu)\, \cos 2\pi\nu x \,, \\ I_1 &:= \frac{1}{\pi\sqrt{\mathcal{D}}} \sum_{m=-\infty}^{\infty} \frac{x-m}{\sqrt{\mathcal{D}}} \operatorname{sech} \frac{x-m}{\sqrt{\mathcal{D}}} \\ &= \pi \sum_{\nu=1}^{\infty} \operatorname{sech}(\pi^2\sqrt{\mathcal{D}}\nu) \tanh(\pi^2\sqrt{\mathcal{D}}\nu)\, \sin 2\pi\nu x \,, \end{aligned}$$

which shows that

$$|I_0 - 1| < 2\varepsilon(\mathcal{D}) \quad \text{and} \quad |I_1| < \pi\varepsilon(\mathcal{D}) \,,$$

where we use the notation

$$\varepsilon(\mathcal{D}) := \sum_{\nu=1}^{\infty} \operatorname{sech}(\pi^2\sqrt{\mathcal{D}}\nu) \,.$$

Moreover,

$$\frac{1}{2\pi\sqrt{\mathcal{D}}} \left| \sum_{m=-\infty}^{\infty} u''(x_m) \frac{(mh-x)^2}{\mathcal{D}h^2} \operatorname{sech} \frac{x-mh}{\sqrt{\mathcal{D}}h} \right| \le \frac{5}{4} \sup_{t\in\mathbb{R}} |u''(t)| \,,$$

so that

$$|u(x) - \mathcal{M}_h u(x)| \le \frac{5}{4} \mathcal{D}h^2 \max_{\mathbb{R}} |u''| + \varepsilon(\mathcal{D}) \big(2\ |u(x)| + \pi\sqrt{\mathcal{D}}h\, |u'(x)| \big) \,. \tag{1.22}$$

As in the example with the Gaussian function the quasi-interpolant (1.21) does not converge to $u(x)$, but the number $\varepsilon(\mathcal{D})$ is an upper bound for the saturation error and can be made arbitrarily small by choosing $\mathcal{D}$ large enough. For example, if $\mathcal{D} = 4$, then $\varepsilon(\mathcal{D}) = 0.000000005351$.

Again, the inequality (1.22) shows that the quasi-interpolant $\mathcal{M}_h u$ approximates any C^2-function u like a second-order approximant above the tolerance

$$\varepsilon(\mathcal{D}) \big(2\, |u(x)| + \pi\sqrt{\mathcal{D}}h\, |u'(x)| \big) \,,$$

and that any prescribed accuracy can be reached if $\mathcal{D}$ is chosen sufficiently large. In Table 1.3 we give the L^∞-error of the quasi-interpolation of $\sin x$ with formula (1.22) for different h and $\mathcal{D}$ and the convergence rate obtained using (1.14).

1.2.4. Examples of higher-order quasi-interpolants. There exist approximants with approximation orders larger than 2 up to some prescribed accuracy which have the same simple form as second-order approximate quasi-interpolants. Consider, for example, the quasi-interpolant

$$u_h(x) := \mathcal{D}^{-1/2} \sum_{m=-\infty}^{\infty} u(mh)\, \eta\Big(\frac{x-mh}{\sqrt{\mathcal{D}}h} \Big) \tag{1.23}$$

h	$\mathcal{D}=1$	rate	$\mathcal{D}=2$	rate	$\mathcal{D}=4$	rate
0.4	$1.69\cdot 10^{-1}$		$2.96\cdot 10^{-1}$		$4.73\cdot 10^{-1}$	
0.2	$4.75\cdot 10^{-2}$	1.83	$9.12\cdot 10^{-2}$	1.70	$1.69\cdot 10^{-1}$	1.48
0.1	$1.24\cdot 10^{-2}$	1.93	$2.42\cdot 10^{-2}$	1.92	$4.74\cdot 10^{-2}$	1.84
0.05	$3.32\cdot 10^{-3}$	1.91	$6.14\cdot 10^{-3}$	1.98	$1.22\cdot 10^{-2}$	1.96
0.025	$1.01\cdot 10^{-3}$	1.71	$1.54\cdot 10^{-3}$	1.99	$3.08\cdot 10^{-3}$	1.99
0.0125	$4.37\cdot 10^{-4}$	1.22	$3.89\cdot 10^{-4}$	1.99	$7.71\cdot 10^{-4}$	2.00
0.00625	$2.18\cdot 10^{-4}$	1.01	$9.98\cdot 10^{-5}$	1.96	$1.93\cdot 10^{-4}$	2.00

TABLE 1.3. Error of approximating $u(x)=\sin x$ with formula (1.21)

with one of the two generating functions

$$\eta_1(x)=(3/2-x^2)\,\frac{\mathrm{e}^{-x^2}}{\sqrt{\pi}} \quad \text{or} \quad \eta_2(x)=\sqrt{\frac{\mathrm{e}}{\pi}}\;\mathrm{e}^{-x^2}\cos\sqrt{2}x\,, \tag{1.24}$$

shown in Figs. 1.19 and 1.20.

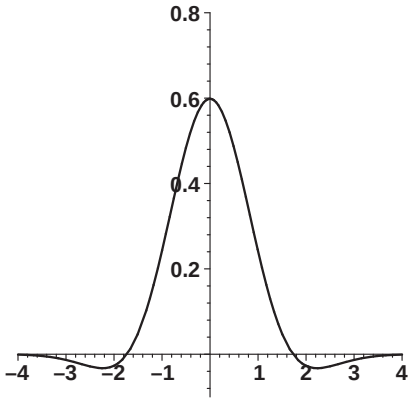

FIGURE 1.19. $\eta_1(x/\sqrt{2})$

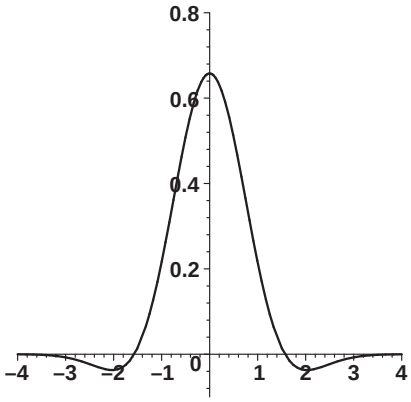

FIGURE 1.20. $\eta_2(x/\sqrt{2})$

Figs. 1.21 – 1.26 repeat the error plots of Subsection 1.2.1 for the approximation of the function $\sin x$ with

$$\mathcal{N}_{h,\mathcal{D}}(\mathbf{x}):=\Big(\frac{\mathrm{e}}{\pi\mathcal{D}}\Big)^{1/2}\sum_{m=-\infty}^{\infty}u(mh)\,\cos\big(\sqrt{2/\mathcal{D}}(x/h-m)\big)\;\mathrm{e}^{-(x-mh)^2/\mathcal{D}h^2}\,, \tag{1.25}$$

where now the values $\mathcal{D}=1.5$ and $\mathcal{D}=2.5$ are used.

The absolute errors given in Figs. 1.21 and 1.22 are much smaller than those plotted in Figs. 1.8 and 1.9. Moreover, the graphs indicate approximation with the order 4.

The visible oscillations of the errors in Fig. 1.21 (the case $\mathcal{D}=1.5$ for quite large steps h) are caused by the relatively large saturation error. The error plots in Figs. 1.23 and 1.25 show clearly that $\mathcal{N}_{0.1,1.5}$ has reached the saturation and that

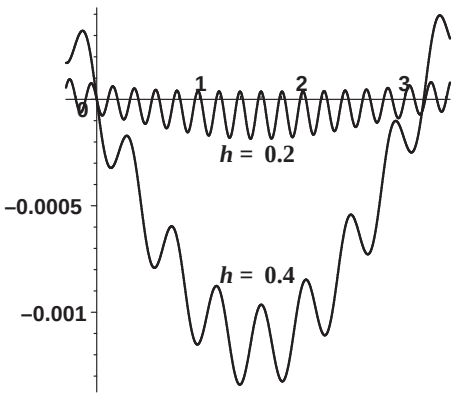

FIGURE 1.21. $(\mathcal{N}_{h,1.5} - I)\sin x$

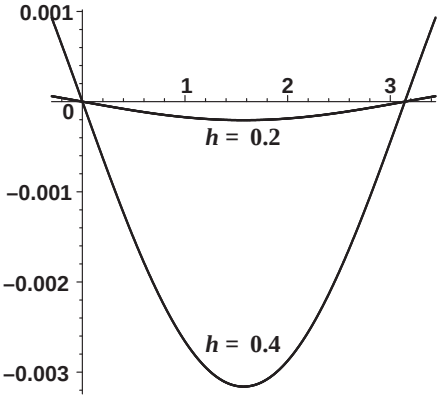

FIGURE 1.22. $(\mathcal{N}_{h,2.5} - I)\sin x$

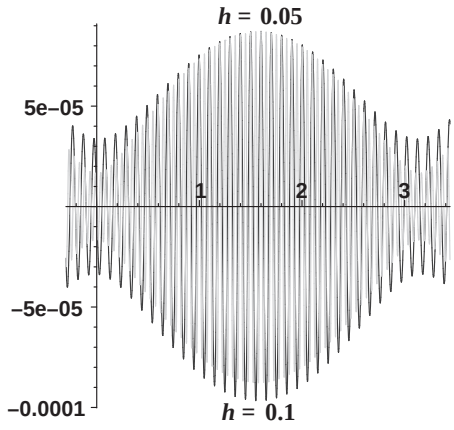

FIGURE 1.23. $(\mathcal{N}_{h,1.5} - I)\sin x$

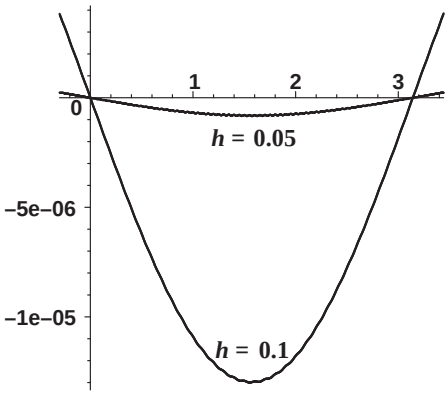

FIGURE 1.24. $(\mathcal{N}_{h,2.5} - I)\sin x$

any h smaller than 0.1 does not give more accurate results for the quasi-interpolant $\mathcal{N}_{h,1.5}$.

The situation is much better for $\mathcal{N}_{h,2.5}$, as indicated in Figs. 1.24 and 1.26. The approximation is much more accurate for small h; the approximation error is dominated by the saturation only if $h \leq 0.01$.

The approximation errors of the function $\sin x$ with the basis functions (1.24) are given in the Tables 1.4 and 1.5 which confirm an approximation with the order 4 up to some saturation error.

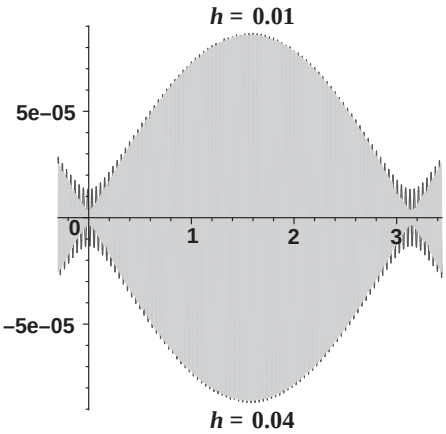

FIGURE 1.25. $(\mathcal{N}_{h,1.5} - I)\sin x$

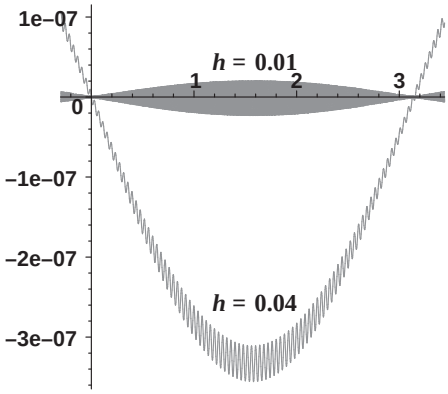

FIGURE 1.26. $(\mathcal{N}_{h,2.5} - I)\sin x$

h	$\mathcal{D}=2$	ord	$\mathcal{D}=3$	ord	$\mathcal{D}=4$	ord
0.4	$3.03\cdot10^{-3}$		$6.65\cdot10^{-3}$		$1.15\cdot10^{-2}$	
0.2	$1.97\cdot10^{-4}$	3.85	$4.41\cdot10^{-4}$	3.76	$7.79\cdot10^{-4}$	3.70
0.1	$1.26\cdot10^{-5}$	3.92	$2.80\cdot10^{-5}$	3.94	$4.97\cdot10^{-5}$	3.92
0.05	$8.96\cdot10^{-7}$	3.51	$1.75\cdot10^{-6}$	3.99	$3.12\cdot10^{-6}$	3.98
0.025	$1.60\cdot10^{-7}$	1.39	$1.09\cdot10^{-7}$	4.00	$1.95\cdot10^{-7}$	4.00
0.0125	$9.72\cdot10^{-8}$	0.41	$7.63\cdot10^{-9}$	3.98	$1.24\cdot10^{-8}$	4.03

TABLE 1.4. Error of approximating $u(x)=\sin x$ with $\eta(x)=\dfrac{3/2-x^2}{\pi^{1/2}}\,\mathrm{e}^{-x^2}$

h	$\mathcal{D}=2$	ord	$\mathcal{D}=3$	ord	$\mathcal{D}=4$	ord
0.4	$2.04\cdot10^{-3}$		$4.50\cdot10^{-3}$		$7.84\cdot10^{-3}$	
0.2	$1.34\cdot10^{-4}$	3.81	$2.95\cdot10^{-4}$	3.81	$5.22\cdot10^{-4}$	3.75
0.1	$9.94\cdot10^{-6}$	3.37	$1.87\cdot10^{-5}$	3.95	$3.32\cdot10^{-5}$	3.94
0.05	$2.00\cdot10^{-6}$	1.24	$1.17\cdot10^{-6}$	3.99	$2.08\cdot10^{-6}$	3.98
0.025	$1.48\cdot10^{-6}$	0.34	$7.43\cdot10^{-8}$	3.97	$1.30\cdot10^{-7}$	4.00
0.0125	$1.33\cdot10^{-6}$	0.28	$5.38\cdot10^{-9}$	3.65	$8.42\cdot10^{-9}$	4.07

TABLE 1.5. Error of approximating $u(x)=\sin x$ with $\eta(x)=\dfrac{\mathrm{e}^{1/2-x^2}}{\pi^{1/2}}\cos\sqrt{2}x$

We see in Section 3.3, Example 3.2, that

$$\eta_{10}(x)=\pi^{-1/2}\,\mathrm{e}^{-x^2}\left(\frac{315}{128}-\frac{105}{16}\,x^2+\frac{63}{16}\,x^4-\frac{3}{4}\,x^6+\frac{1}{24}\,x^8\right) \tag{1.26}$$

generates a quasi-interpolant which approximates smooth functions with the order $N = 10$ up to some small saturation. This theoretical result is confirmed in Table 1.6.

h	$\mathcal{D} = 3$	ord	$\mathcal{D} = 5$	ord	$\mathcal{D} = 6$	
0.8	$1.41 \cdot 10^{-4}$		$1.41 \cdot 10^{-3}$		$3.08 \cdot 10^{-3}$	
0.7	$4.17 \cdot 10^{-5}$	9.11	$4.33 \cdot 10^{-4}$	8.85	$9.74 \cdot 10^{-4}$	8.62
0.6	$1.00 \cdot 10^{-5}$	9.24	$1.06 \cdot 10^{-4}$	9.13	$2.45 \cdot 10^{-4}$	8.96
0.5	$1.87 \cdot 10^{-6}$	9.22	$1.92 \cdot 10^{-5}$	9.38	$4.53 \cdot 10^{-5}$	9.25
0.4	$3.03 \cdot 10^{-7}$	8.16	$2.26 \cdot 10^{-6}$	9.58	$5.44 \cdot 10^{-6}$	9.50
0.3	$6.68 \cdot 10^{-8}$	5.26	$1.37 \cdot 10^{-7}$	9.75	$3.34 \cdot 10^{-7}$	9.70
0.2	$2.67 \cdot 10^{-8}$	2.26	$2.57 \cdot 10^{-9}$	9.80	$6.20 \cdot 10^{-9}$	9.83
0.1	$1.39 \cdot 10^{-8}$	0.94	$7.52 \cdot 10^{-11}$	5.10	$2.07 \cdot 10^{-11}$	8.29
0.05	$1.12 \cdot 10^{-8}$	0.31	$7.12 \cdot 10^{-11}$	0.07	$8.52 \cdot 10^{-12}$	1.34

TABLE 1.6. Error of approximating $u(x) = \sin x$ with the basis function (1.26)

1.2.5. Examples of multi-dimensional quasi-interpolants. One important feature of approximate quasi-interpolation is the simplicity of its multi-dimensional generalization. In the next chapters, we shall see that sufficiently smooth and rapidly decaying functions with non-vanishing mean value can be taken as generating functions for quasi-interpolants on uniform grids in $\mathbb{R}^n$. So we have access to a large class of appropriate functions, which generate high-order approximants with simple analytic representations. This is, for example, in contrast to the case of spline functions, where n-dimensional generalizations have quite complicated analytic expressions.

One possibility is, for example, to use the radial counterparts of one-dimensional generating functions. So the n-dimensional analogue of (1.7) is the formula

$$\mathcal{M}_{h,\mathcal{D}} u(\mathbf{x}) = \frac{1}{(\pi\mathcal{D})^{n/2}} \sum_{\mathbf{m}\in\mathbb{Z}^n} u(h\mathbf{m})\, \mathrm{e}^{-|\mathbf{x}-h\mathbf{m}|^2/\mathcal{D}h^2}\,, \tag{1.27}$$

whereas (1.21) can be extended to the approximation formula

$$\frac{1}{c_n \mathcal{D}^{n/2}} \sum_{\mathbf{m}\in\mathbb{Z}^n} u(h\mathbf{m}) \operatorname{sech} \frac{|\mathbf{x}-h\mathbf{m}|}{\sqrt{\mathcal{D}}h}\,, \quad c_n = \int_{\mathbb{R}^n} \operatorname{sech}|\mathbf{x}|\, d\mathbf{x}\,.$$

Here and in what follows we make the notational convention that finite-dimensional vectors are denoted by bold face symbols, i.e., $\mathbf{x} = (x_1, \ldots, x_n) \in \mathbb{R}^n$, $\mathbf{m} = (m_1, \ldots, m_n)$, $m_j \in \mathbb{Z}$. The scalar product of two vectors $\mathbf{x} = (x_1, \ldots, x_n)$ and $\mathbf{y} = (y_1, \ldots, y_n)$ in the Euclidean space $\mathbb{R}^n$ is denoted by

$$\langle \mathbf{x}, \mathbf{y} \rangle = \sum_{j=1}^{n} x_j y_j\,.$$

For the Euclidean norm of $\mathbf{x} \in \mathbb{R}^n$, we use the notation

$$|\mathbf{x}| = |\mathbf{x}|_2 = \sqrt{\langle \mathbf{x}, \mathbf{x} \rangle}\,.$$

We shall see in the next chapter that both formulas approximate with order $\mathcal{O}(h^2)$ up to some saturation bound.

A fourth-order approximation up to some small saturation is given by the formula

$$\frac{1}{(\pi\mathcal{D})^{n/2}} \sum_{\mathbf{m}\in\mathbb{Z}^n} u(\mathbf{m}h)\Big(\frac{n+2}{2} - \frac{|\mathbf{x}-\mathbf{m}h|^2}{\mathcal{D}h^2}\Big)\, \mathrm{e}^{\,-|\mathbf{x}-h\mathbf{m}|^2/\mathcal{D}h^2}$$

whereas the sixth-order can be obtained with the generating function

$$\eta(\mathbf{x}) = \frac{\mathrm{e}^{-|\mathbf{x}|^2}}{2\pi^{n/2}}\Big(\frac{(n+4)(n+2)}{4} - (n+4)|\mathbf{x}|^2 + |\mathbf{x}|^4\Big).$$

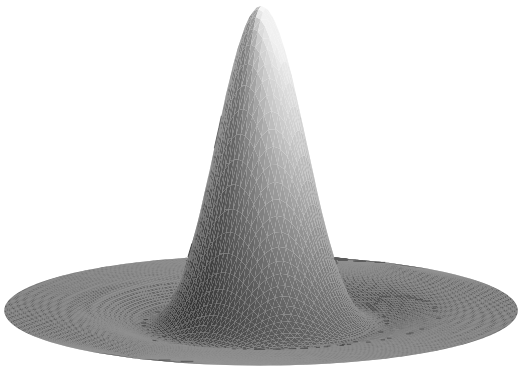

FIGURE 1.27. Sixth-order generating function in $\mathbb{R}^2$

Furthermore, in some applications, we use generating functions of the form

$$\eta(\mathbf{x}) = \phi(\langle A\mathbf{x}, \mathbf{x}\rangle)\,,$$

where A is an $n \times n$ matrix.